Analysis of Forward Scattering Data for Microwave Breast Imaging

Analysis of Forward Scattering Data for Microwave Breast Imaging

Hoi-Shun Lui [#], Andreas Fhager[#], Mikael Persson [#]

[#]*Department of Signals and Systems, Chalmers University of Technology*
SE-412 96, Gothenburg, Sweden
[#]antony.lui@chalmers.sem

***Abstract* — Microwave imaging for breast cancer detection has been of significant interest for the last two decades. Recent studies focus on solving the imaging problem using an inverse scattering approach. Success of these methods relies on the quality of the forward data such that the tumor inside the breast volume is well illuminated. In this paper, a numerical study of the forward scattering data is conducted and the potential use of full polarimetric data is investigated.**

***Index Terms* — Microwave Imaging, Breast Cancer Detection, Ultra Wideband, Polarization, Inverse Problem.**

I. INTRODUCTION

In the last two decades, extensive studies have been contributed to breast cancer detection using microwave based technology. Compare to X-ray mammography which is widely used in hospital nowadays for breast cancer detection, microwave is a non-ionizing radiation which is safer to patient. Early studies (e.g. [1]) have reported that there is a huge contrast between malignant tumor and healthy breast tissue which forms a strong foundation for the use of microwave based techniques for breast cancer detection, although recent studies [2]-[3] have reported that the contrast is much lower. This has raised an issue of whether malignant tumor can be detected, especially when the relative permittivity of the tumor is close to that of the surrounding tissue.

In general, studies on microwave breast cancer detection can be divided mainly into two main groups, namely the radar-based imaging approach (e.g. [1]) and the inverse scattering approach [4]-[6]. Here we mainly focus on the inverse scattering approach. The objective of inverse scattering is to reconstruct the unknown dielectric profiles of the target, i.e. the breast volume. First, the multi-static measurement from the breast volume is taken as reference. Based on numerical solutions of the Maxwell's equations (e.g. Finite-Difference Time-Domain (FDTD) [7]), the entire volume can be spatially discretized into a number of variables with unknown dielectric properties (Yee cells for FDTD). The corresponding forward problems with the same transmitter/receiver configuration are included and the computation can be done with an initial guess of the dielectric profiles of the breast volume. Given the reference data from the "actual" breast volume and the simulated data from the "assumed" breast volume, a cost function based on the differences between these two data sets is defined [4]-[5]. The cost function is then minimized in an iterative manner by changing the dielectric properties in each Yee cell in the modeling domain using a gradient-based optimization. Assuming that the global minima is reached at the end of the optimization, i.e. the simulated data is almost the same or even identical to the reference data, the resulting dielectric profiles in the simulation domain is thus the resultant image provide that the global minima is reached [4]-[5].

Image reconstruction process is an ill-posed multi-dimensional optimization problem that the number of unknown variables ($\varepsilon_r(x,y,z), \sigma(x,y,z)$) depends mainly on the physical size, required spatial resolution, dielectric properties of the geometry and the frequency of interest of the problem. Optimization of such a high dimensional problem with thousands unknown variables is not trivial and chances for trapping into local minima could be high.

Furthermore, the uniqueness of the solution is also important. Given a set of measured data, there could be more than one distribution of dielectric profiles that can result in the same or similar measured data. As an example, if we consider some early studies in the literature [8] that compares the mono-static Ultra Wideband (UWB) response from the breast volume with and without tumor, it is found that the differences between the co-polarized components of the two cases is lower than that of the cross-polarized components. In other words, it is difficult to tell if there is any tumor by looking at the co-polarized response, but the contrast is more apparent if the cross-polarized response is considered.

The use of polarization diversity has been widely used for radar imaging applications. The transmitters and receivers are located in the far-field region such that higher-order interactions between the target and the transmitters as well as targets and receivers can be ignored. Mutual coupling between transmitters and receivers antennas can be also ignored in the forward scattering scenario and thus the measured response is purely target dependent. In microwave breast imaging scenario, the breast volume is surrounded by an antenna array in the near-field region and thus mutual coupling between antenna elements as well as higher order interactions between the breast volume and the antennas are significant. To reduce the reflection from the skin-air interface, the breast volume is usually immersed into some matching liquid. A possible exemption could be the case if the operation frequency is high enough such that the antenna is electromagnetically far from the breast and the conductivity of the matching liquid is high such that higher-order interactions are attenuated. Due to the above complexities in the near field region, polarimetric microwave breast imaging has not been well exploited. In most cases, the co-polarized responses of the breast volume under linear polarization basis are considered in the image reconstruction process.

In this paper, the possibilities of using polarimetric information for microwave breast imaging are considered. In particular, the forward scattering data of the two cases, i.e. breast volume with and without tumor, under different polarization basis is investigated. The objective here is to investigate if better contrast of the forward data can be obtained such that the two cases are more distinguishable. With two distinguishable sets of forward data, chances for the two inverse problems heading to the same solution in the optimization process could be reduced. To simplify the analysis, homogenous breast volume together with scattered far-field under different polarization basis is considered. The motivations behind the simplified models and setup are given as follows.

i) We would like to see if the scattering problem itself under a different polarization basis can result in better contrast of the data that can be used for solving the inverse problem. This is the most fundamental data as it is purely dependent to the target i.e. the breast volume. If antenna elements are included, higher-order interactions cannot be ignored and such interactions vary as a function of frequency, antenna positions and the choice of antenna elements, which is difficult to analyze.

(ii) Traditionally, polarization is treated in the far-field region in frequency domain. Although the corresponding near-field components in the Cartesian or polar coordinates can be computed, the concept of polarization in the near field region is not well defined.

II.UWB SCATTERING OF BREAST VOLUME UNDER DIFFERENT POLARIZATION STATES

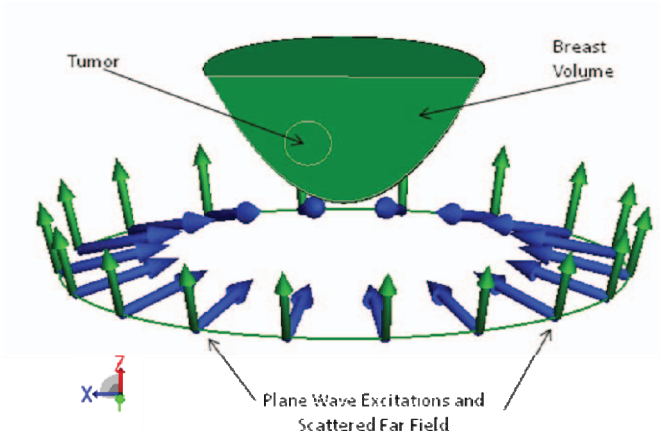

Fig. 1. The Breast volume under plane wave illumination

Here, we would like to mimic the microwave breast imaging setup as described in [4]. The breast volume is placed inside a circular array with 14 to 18 monopole antenna elements. The breast volume is illuminated with 1 antenna acting as transmitter and the other antennas acting as receivers such that a projection of the breast volume is obtained. Each antenna element of the array takes turn and the projections of the breast volume from different angles are obtained. Image reconstruction is performed based on these data sets. Regarding the operation frequency, a UWB approach is taken.

The breast volumes shown in Fig. 1 are considered. It is a hemisphere with radius of 6cm. The entire breast volume is illuminated from 23MHz to 3GHz with 128 samples in frequency domain. The relative permittivity of the breast tissue is $\varepsilon_r = 5$ is used which are taken from the Cole-Cole-4 model of fat tissue presented in Gabriel et al. [9]. To simulate the breast imaging scenario without using actual antenna elements which would complicate the entire electromagnetic problem, the elevation angle of $\theta = 105°$ is considered ($\theta = 0°$ corresponds to the positive z axis) and the incident plane wave together with the corresponding scattered far-field at 18 different directions are equally spaced within the circle (i.e. 20° separation). Both forward and back scattering are considered. For instance, for the plane wave excitation coming from $\theta = 105°$, $\phi = 40°$ ($\phi = 0°$ corresponds to the positive x axis), the scattered far field at the directions of $\theta = 105°$, $\phi = 0°$, 20°, 40°, 60°,…, 320° and 340° are determined. The computation is done using commercial moment method solver FEKO in frequency domain [10].

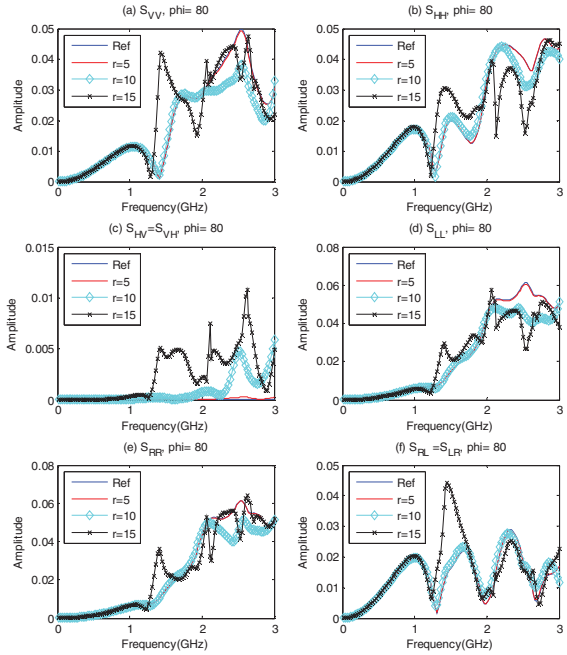

Fig. 2. Monostatic response from breast volumes in frequency domain at $\theta = 105°$ $\phi = 80°$. (a) S_{VV}; (b) S_{HH}, (c) $S_{HV} = S_{VH}$ (d) S_{LL}, (e) S_{RR} and (f) $S_{RL} = S_{LR}$

As an example, the monostatic amplitude responses of the breast volume at $\phi = 80°$ in frequency domain under different polarization states are shown in Fig. 2 in blue lines (Ref, but mostly overlapped with red lines, see below), which are the reference case in this study. Both linear and circular polarization states are considered. The results in Fig.2 are essentially the components scattering matrix as a function of

frequency, i.e. $[S]=\begin{bmatrix} S_{xx}(f) & S_{xy}(f) \\ S_{yx}(f) & S_{yy}(f) \end{bmatrix}$, where the first subscript (x or y) in each term in the matrix corresponds to the transmitting polarization state and the second subscript corresponds to the receiving polarization state. Vertical (V) and horizontal (H) are utilized for linear while Left-Handed (L) and Right-Handed (R) are used for circular polarization basis. Under monostatic configurations, $S_{VH}=S_{HV}$ and $S_{LR}=S_{RL}$. Due to the geometrical symmetric nature, $S_{VH}=S_{HV}$ and they are null. To simulate the case with a tumor, a dielectric sphere with the relative permittivity of $\varepsilon_r=50$, centres at the position of ($15mm$, $15mm$, $30mm$), is introduced. Three cases with different radius of the spheres, $5mm$, $10mm$ and $15mm$ are considered and the corresponding amplitude responses plotted in red, cyan and black respectively in Fig. 2.

At frequencies below 1GHz, it is observed in Fig. 2 that the amplitude responses for the 4 breast volumes are similar for the two linear co-polarized and the four circular polarized states. It is apparent that for the case with 15mm tumor, the amplitude response is different to the other three cases for frequency above 2GHz. For the case with 10mm tumor, there are larger amplitude differences at ~2.5GHz for S_{VV}, S_{VH}, S_{LL} and S_{RR} than S_{HH} and S_{LR} when comparing with the 5mm tumor case and no tumor case. The results for the case with 5mm tumor (red) are almost the same to the reference data which is difficult to distinguish by looking the frequency responses. Overall, the results indicate that the amplitude responses could be more distinguishable in some polarimetric states than the other.

Consider the configuration that involves a large amount of data ($N_{tx}=N_{rx}=18$ and 8 polarization states), visual inspection is not feasible in practice. In view of this, we quantify the percentage differences of the amplitude response when a tumor is introduced with respect to the reference case without tumor. The relative difference between each frequency sample can be given by

$$S_{xy,diff}(f,tx,rx)=\frac{\left|\left|S_{xy,ref}(f,tx,rx)\right|-\left|S_{xy,tumor}(f,tx,rx)\right|\right|}{\left|S_{xy,ref}(f,tx,rx)\right|}\times 100\% \,. \quad (1)$$

To quantify the difference of the data at different transmitter/receiver configurations, the "mean differences" of the data at each transmitter and receiver directions, MD_{xy}, can be given by

$$MD_{xy}(tx,rx)=\left[\sum_{f=\Delta f}^{N\Delta f} S_{xy,diff}(f,tx,rx)\right]\Big/ N \,. \quad (2)$$

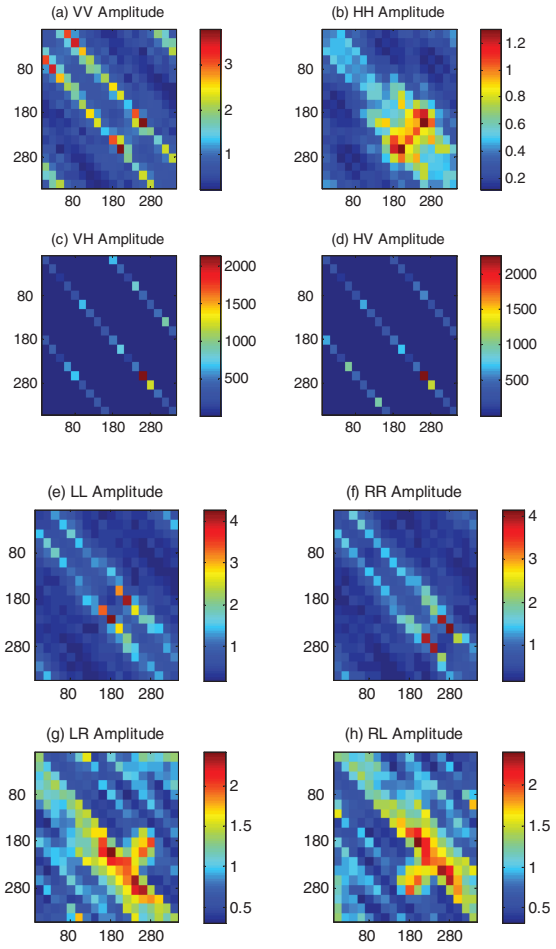

Fig. 3. MD_{xy} for different transmitter/receiver combination. The comparison is made between the reference data (no tumor) with the case with 5mm tumor. (a) VV, (b) HH, (c) HV, (d)VH, (e) LL, (f) RR, (g) RL and (h) LR. The vertical and horizontal axes correspond to the aspects of the incidence ($\phi=0°$ to $340°$) and the aspects of the scattered far-field ($\phi=0°$ to $340°$).

The results for comparison between the cases of 5mm tumor with the reference data are shown in Fig. 3(a) to (h). It can be observed that MD_{xy} vary as the transmitter/receiver configurations change. The MD s for VV, HH and the circular polarization basis are less than 4% and more than 100% of MD s are observed for the VH and HV. Such high values for VH and HV are due to the fact that the cross polarized components for the case without tumor is almost zero due to the geometrical symmetry. In reality, due to the heterogeneous nature of human tissue, such high values cannot be achieved. On the other hand, it is interesting to observe that high values of MD occur at the diagonal axis, which corresponds to the back scattered direction.

Lastly, to get an overall picture about the differences of the amplitude response for each polarization states, the mean values of MD_{xy}, denoted as MMD_{xy}, can be given by

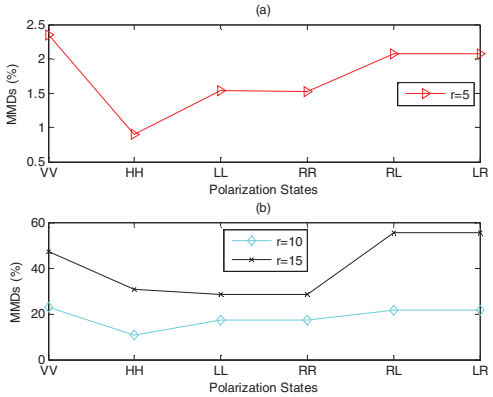

Fig. 4. MMD_{xy} for different polarization states with (a) 5mm, (b) 10mm and 15mm tumor

$$MMD_{xy} = \left[\sum_{rx=0°}^{340°}\sum_{tx=0°}^{340°} MD_{xy}(tx,rx)\right] \Big/ \left[N_{tx} \times N_{rx}\right]. \qquad (3)$$

The corresponding results are shown in Fig. 4 (a) and (b) for 5mm, as well as 10mm and 15mm tumor respectively. It is found that the MMD_{xy} values are relatively small (<2.5%) for the case of 5mm tumor, and increase as the tumor becomes larger (15 to 55%). It is interesting to see that larger difference can be found when the VV, RL and LR polarization states are considered. While not shown in Fig. 4, the results for the two cross-polarized components, HV and VH, are more than 1000% for all cases. Once again this is due to the null cross polarized response for the case without tumor and in practice such values cannot be obtained.

III. DISCUSSION AND CONCLUSIONS

UWB forward scattering data from breast volumes with different tumor sizes are studied. Based on the configurations in this paper, several points can be summarized. To achieve good contrast of the amplitude responses between the cases with and without tumor, the excitation frequency should be at least 1GHz as the lower frequency components correspond mainly to the scattering from the entire breast volume. Second, it is also found that there are higher contrast in the back scattered direction in general. Furthermore, the forward scattering problems under different polarization states and basis are studied. As expected, the VH and HV components have the highest contrast due to the geometrical symmetry when there is no tumor inside the breast volume. Regarding other polarization states, the LR, RL and VV states give better contrast than the LL and RR states. Potentially, cross-polarized components in both linear and circular polarization basis can be employed to obtain data with higher contrast.

This work presented here opens the door for further investigations of better data sets for the microwave breast imaging by considering different polarization states and basis. Although the setup is relatively simple and ideal with lossless homogenous breast volume and high contrast between tumor and tissue (10 times), surprisingly it is found that the existence of small tumor (r=5mm) is not highly revealed in the forward data. Better contrast could be obtained with higher excitation frequency, but the conductivity of breast tissue increases which cannot be ignored [11]. This work essentially is the first step and future work needs to focus on practical issues such as the choice of polarization states, antenna elements, array configurations and matching liquid, and at the same time taken into consideration of realistic breast model that takes care of the heterogeneous nature of the tissue and the contrast between the tumor and breast tissue.

ACKNOWLEDGEMENT

This work was supported by the Swedish Research Council under grant number 2010-7262-78830-59.

REFERENCES

[1] X. Li and S. C. Hagness, "A confocal microwave imaging algorithm for breast cancer detection," *IEEE Microwave and Wireless Components Letters*, vol. 11-3, pp. 130–132, 3 2001.

[2] M. Lazebnik, et al., "A large-scale study of the ultrawideband microwave dielectric properties of normal breast tissue obtained from reduction surgeries," *Physics in Medicine and Biology*, vol. 52, pp. 2637-2656, 2007.

[3] M. Lazebnik, et al., "A large-scale study of the ultrawideband microwave dielectric properties of normal, benign and malignant breast tissues obtained from cancer surgeries," *Physics in Medicine and Biology*, vol. 52, p. 6093-6115, 2007.

[4] A. Fhager, *Microwave tomography*, Ph. D dissertation, Dept. of Signals and Systems, Chalmers University of Technology, Sweden, 2006.

[5] A. Fhager, P. Hashemzadeh and M. Persson, "Reconstruction Quality and Spectral Content of an Electromagnetic Time-domain Inversion Algorithm", *IEEE Trans. Biomedical Engineering*, Vol. 53, No. 8, pp. 1594-1604, July 2006

[6] T. Rubaek, O. S. Kim and P. Meincke, "Computational Validation of a 3-D Microwave Imaging System for Breast-Cancer Screening", *IEEE Trans. Antennas Propag.*, Vol. 57, No. 7, pp. 2105-2115, May 2009

[7] K. Yee, "Numerical solution of initial boundary value problems involving Maxwell's equations in isotropic media". *IEEE Trans. Antennas Propag.* Vol. 14, No. 3, pp.302–307, 1966

[8] J. Zhang and E. C. Fear, "Preliminary Investigation of Breast Tumor Detection using Cross-Vivaldi Antenna,", *Proc. 29th Annual International Conf. of the EMBS*, Sept 2005.

[9] S. Gabriel, R.W. Lau and C. Gabriel, "The dielectric properties of biological tissues: III. Parametric models for the dielectric spectrum, of tissues", *Phys. Med., Biol.*, Vol. 41, no.11, pp. 2271-2293, Nov. 1996

[10] FEKO EM Software & Systems S.A., (Pty) Ltd, 32 Techno Lane, Technopark, Stellenbosch, 7600, South Africa

[11] H. S. Lui and N. V. Z. Shuley, "Detection of Depth Changes of a Metallic Target Buried inside a Lossy Halfspace Using the E-Pulse Technique", *IEEE Trans. Electromagn. Compat.,* Vol. 49, No. 4, pp. 868-875, Nov. 2007.